

1 **Supplementary Materials for “A Refined Understanding of**
2 **the Ice Cloud Longwave Scattering Effects in Climate**
3 **Model”**

4
5 Chongxing Fan^{1*}, Yi-Hsuan Chen¹⁺, Xiuhong Chen¹, Wuyin Lin², Ping Yang³,
6 Xianglei Huang¹

7
8 ¹ Department of Climate and Space Sciences and Engineering, the University of Michigan, Ann Arbor,
9 Michigan, USA

10 ² Environmental & Climate Sciences Department, Brookhaven National Laboratory, New York State, USA

11 ³ Department of Atmospheric Sciences, Texas A&M University, Texas, USA

12
13 * Corresponding Author: Chongxing Fan (cxfan@umich.edu)

14 ⁺ Current affiliation: Research Center for Environmental Changes, Academia Sinica, Taipei, Taiwan

15
16
17
18 Submitted to *Journal of Advanced Modeling Earth Systems*

19 Original submission on November 5, 2022

20 Resubmission on May 7, 2023

21 Revision on August 23, 2023

Contents of this file

Figures S1 to S4.

Introduction

In this short introduction, we discuss the cloud field changes in fully-coupled simulations and prescribed simulations due to cloud LW scattering.

Figure S2 shows the change in cloud ice content ratio due to cloud LW scattering. We define the cloud ice content ratio as the ratio of in-cloud ice mixing ratio (r_{ice}) and in-cloud total water mixing ratio ($r_{total} = r_{ice} + r_{liquid}$). In the fully coupled simulations (first row), we can see a general cloud ice-to-liquid transition all over the globe, but there is a prominent ice-to-liquid transition at approximately 600 hPa in the tropics. The ice content ratio decrease can be up to 20%. We cannot see such a strong effect in the prescribed runs (second row), suggesting that this cloud phase transition is mostly caused by the slow adjustment. Such cloud phase transition is also observed in the response to the 4xCO₂ experiment.

Figure S3 shows the change in vertically-resolved cloud fraction in the deep tropics (20°S ~ 20°N) due to cloud LW scattering. In general, we see a strong cloud fraction reduction at 200 hPa in all cases, and a relatively smaller cloud fraction increase at ~150 hPa. These patterns of high-cloud change are also seen in the 4xCO₂ experiments with a different magnitude (lowest row), i.e., elevated deep convective cloud and reduced anvil cloud coverage. Again, they are also the result of slow adjustments when the cloud LW scattering is included in the model.

Figure S4 shows the low cloud fraction change due to cloud LW scattering. We follow the definition used in climate models, which categorizes clouds with a cloud top pressure > 700 hPa as low clouds. An increase of low cloud fraction by up to ~0.06 is seen over the southeastern tropical Pacific, southern subtropical Atlantic, and Indian Ocean. Those regions are known for the

45 frequent occurrence of stratiform low clouds. These patterns of low cloud increases are similar to
46 the counterpart pattern in the response to the increase of CO₂ predicted by the E3SMv2 model, but
47 the magnitude of change and statistical significance of such changes are notably different.

48

49

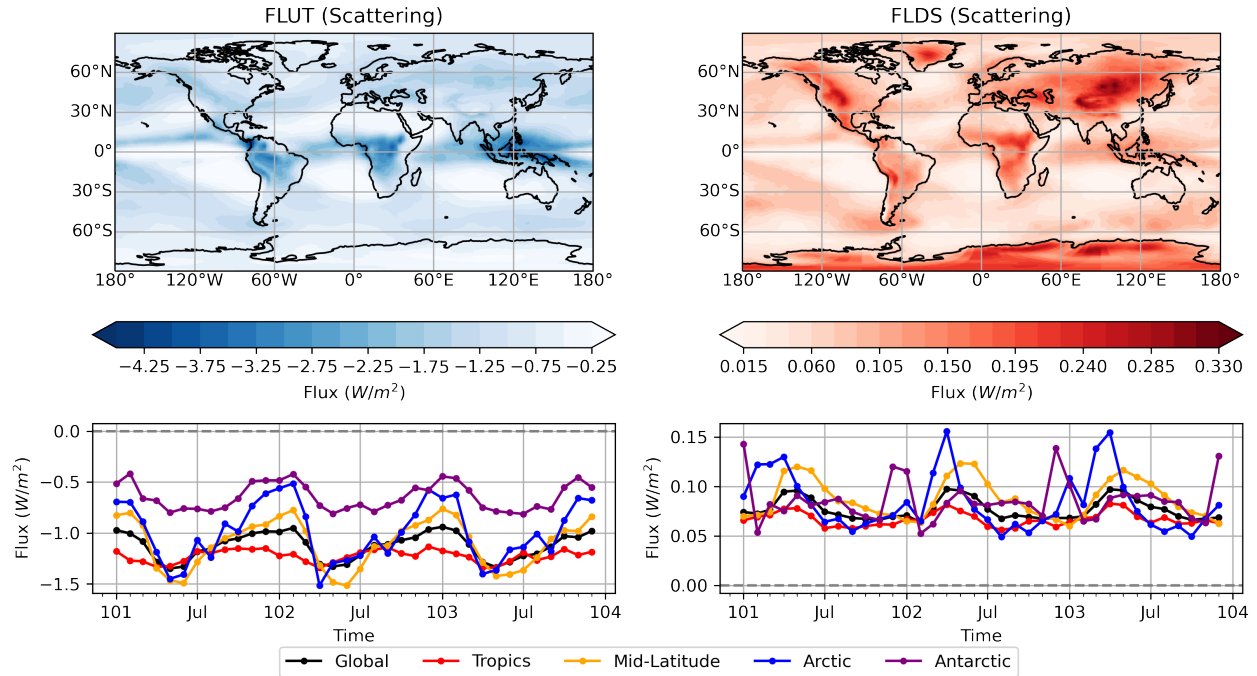
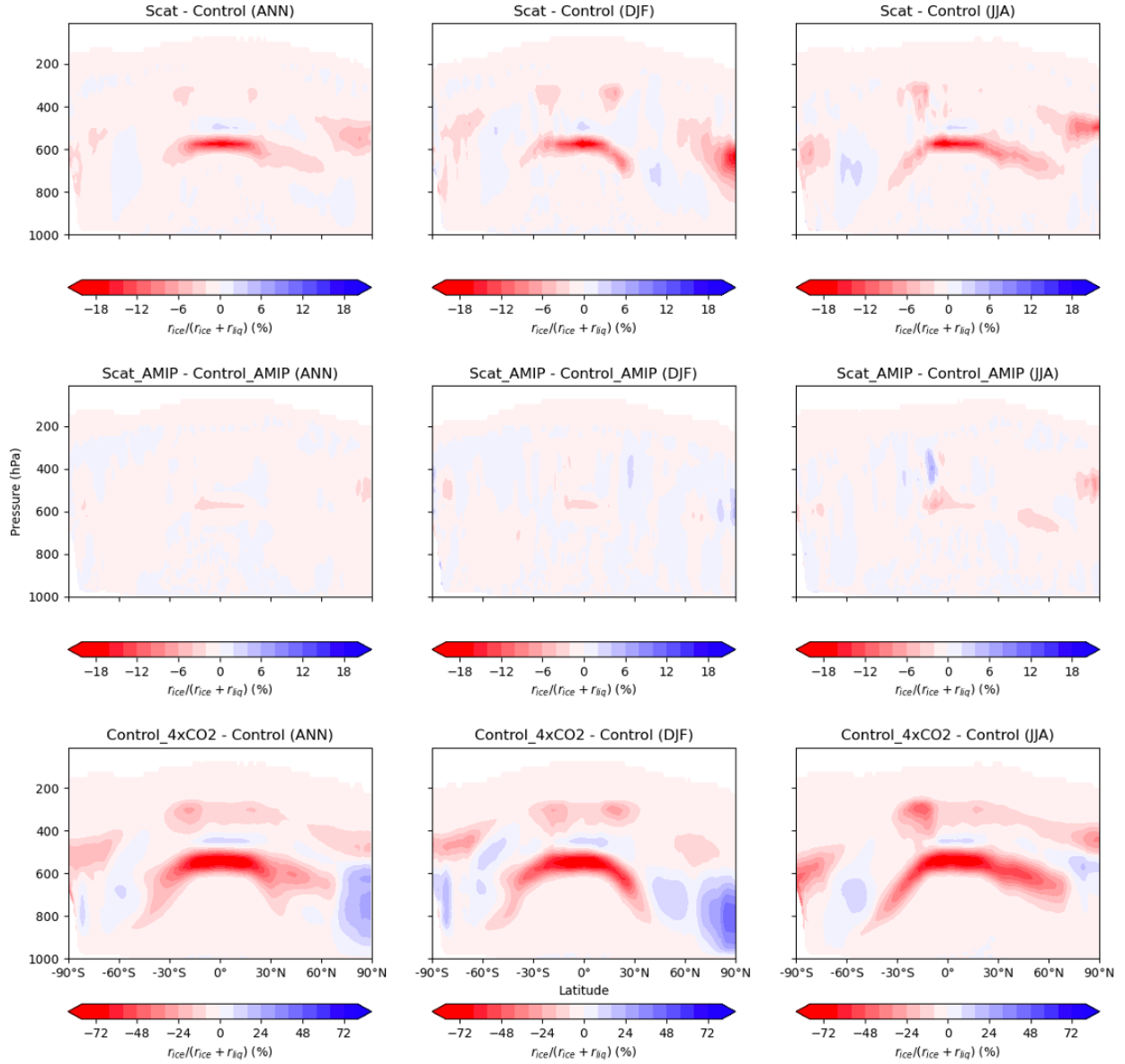


Figure S1. Changes in the upward longwave radiative flux at the top of the atmosphere (FLUT; left column) and the downward longwave radiative flux at the surface (FLDS; right column) due to the direct LW scattering effect. The top row shows the spatial distribution of the three-year mean change, and the bottom row shows the time series of global and regional mean changes in the first three years. Note that the global and regional mean changes have apparent seasonal cycles, but the annually averaged changes vary little from year to year. Each tick on the x-axis of the bottom panels represents a month starting from January of the year 101.



59

60 **Figure S2.** Zonal-mean cloud ice content ratio (i.e., the ratio of in-cloud ice mixing ratio and in-
 61 cloud total water mixing ratio) difference. Negative value (red) means ice-to-liquid transition,
 62 while positive value (blue) means the opposite. The first two rows are the differences resulting
 63 from cloud LW scattering effect in the fully-coupled run and the prescribed run, respectively. The
 64 third row shows the difference resulted from 4xCO₂ concentration. The first column shows the
 65 annual-mean difference, the second column shows the mean difference in boreal winters, and the
 66 third column shows the mean difference in boreal summers.

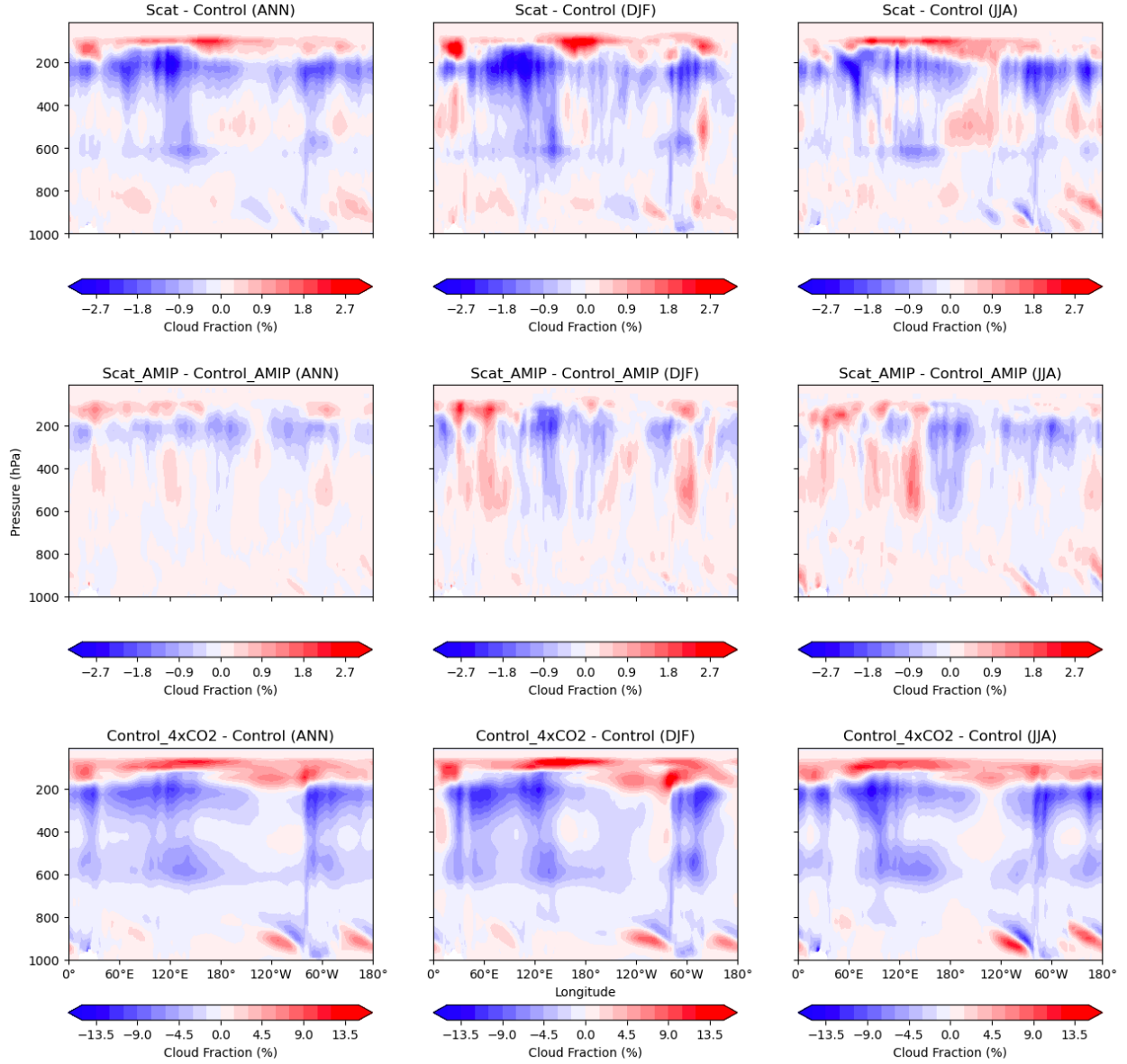


Figure S3. Similar to Figure S2, but this one shows the latitudinal-mean profile difference of the cloud fraction in the deep tropics ($20^{\circ}\text{S} \sim 20^{\circ}\text{N}$). Negative value (blue) indicates less cloud coverage, while positive value (red) indicates the opposite.

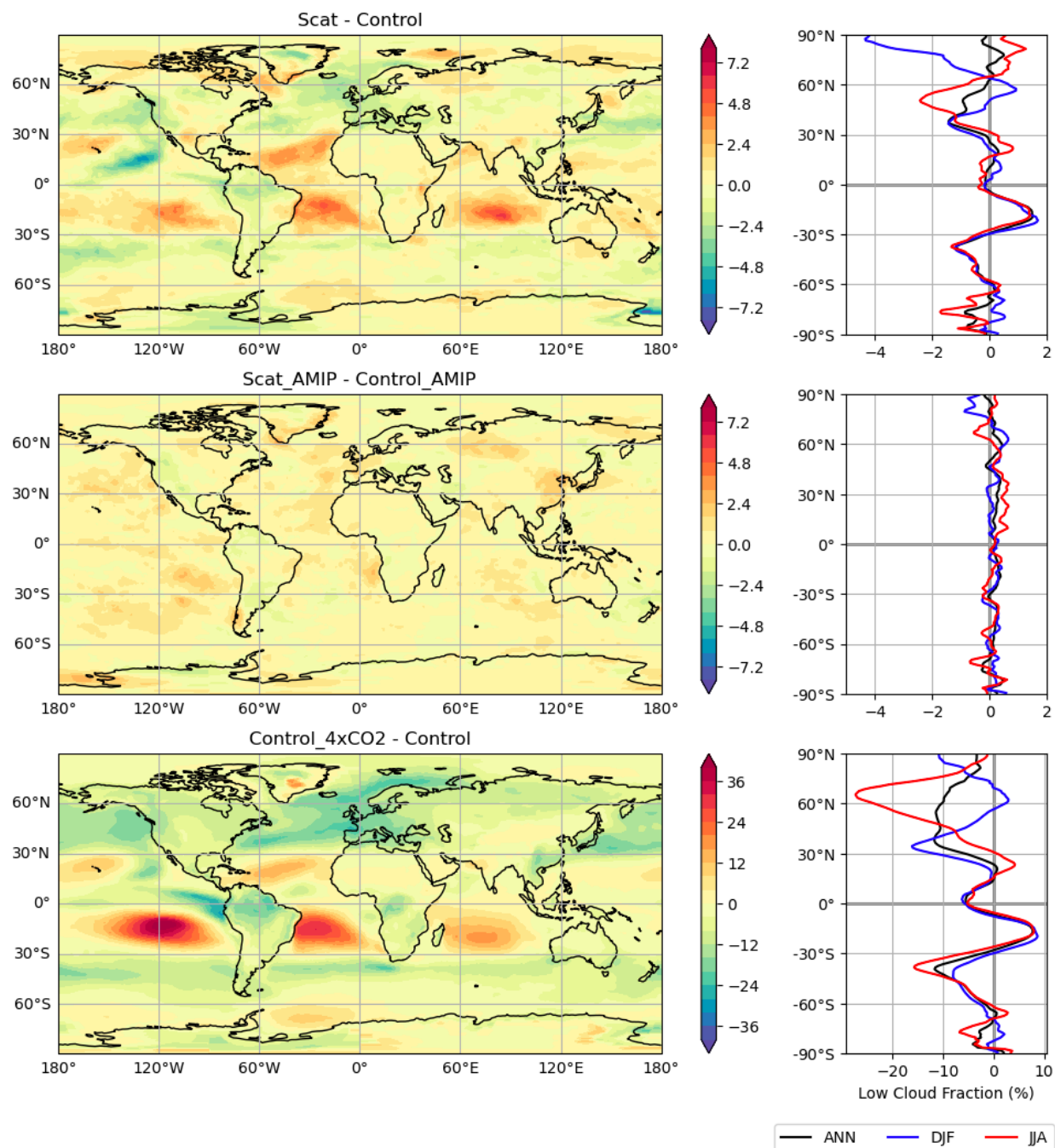


Figure S4. Low cloud fraction change. The first two rows are the differences resulting from cloud LW scattering effect in the fully-coupled run and the prescribed run, respectively. The third row shows the difference resulted from 4xCO₂ concentration. The first column shows the contour map

76 of the annual-mean difference, while the second column shows the zonal-mean difference in all
77 seasons (black), boreal winters (blue), and boreal summers (red).

78